Pinch resonances in a radio-frequency-driven superconducting-quantum-interference-device ring-resonator system

H. Prance, T. D. Clark,* R. Whiteman, R. J. Prance, M. Everitt, and P. Stiffell
Physical Electronics Group, School of Engineering and Information Technology, University of Sussex, Brighton, Sussex BN1 9QT, United Kingdom

J. F. Ralph
Department of Electrical Engineering and Electronics, University of Liverpool, Brownlow Hill, Liverpool L69 3GJ, United Kingdom

(Received 17 February 2000; revised manuscript received 31 January 2001; published 14 June 2001)

In this paper we present experimental data on the frequency domain response of a superconducting-quantum-interference-device ring (a Josephson weak link enclosed by a thick superconducting ring) coupled to a radio frequency tank circuit resonator. We show that with the ring weakly hysteretic the resonance line shape of this coupled system can display opposed fold bifurcations that appear to touch (pinch off). We demonstrate that for appropriate circuit parameters these pinchoff line shapes exist as solutions of the nonlinear equations of motion for the system.

DOI: 10.1103/PhysRevE.64.016208 PACS number(s): 05.45.−a, 47.20.Ky, 85.25.Dq

I. INTRODUCTION

It is well known that the system comprising a superconducting-quantum-interference-device (SQUID) ring (i.e., a single Josephson weak link enclosed by a thick superconducting ring), inductively coupled to a resonant circuit [typically a parallel *LC* radio frequency (rf) tank circuit], can display very interesting dynamical behavior [1–5]. This behavior is due to the nonlinear dependence of the ring screening supercurrent (I_s) on the applied magnetic flux (Φ_x) that originates ultimately from the cosine (Josephson) term in the SQUID ring Hamiltonian [6]. In the past, limitations in the noise level, bandwidth, and dynamic range of rf receivers used to investigate this coupled system have restricted the range of nonlinear phenomena that could be observed, i.e., only relatively weak nonlinearities in $I_s(\Phi_x)$ could be probed. However, recent improvements in rf receiver design have changed this situation quite radically.

The regimes of behavior of SQUID rings [4] are usually characterized in terms of the parameter $\beta=(2\pi\Lambda I_c)/\Phi_o$, where I_c is the critical current of the weak link in the ring, Λ is the ring inductance, and $\Phi_o(=h/2e)$ is the superconducting flux quantum. Thus, when $\beta\leqslant 1$ (the inductive, dissipationless regime) I_s is always single valued in Φ_x. By contrast, for $\beta>1$ (the hysteretic, dissipative regime) this current is multivalued in Φ_x. Both these regimes can lead to very strong nonlinearities in $I_s(\Phi_x)$ [4,5,7]. For the inductive regime these will be strongest when $\beta\rightarrow 1$ from below, at which point I_s becomes almost sawtooth in Φ_x (modulo Φ_o). For the hysteretic regime the existence of bifurcation points in I_s, at particular values of Φ_x, can lead to even stronger nonlinearities. In the absence of external noise these bifurcations, linking adjacent branches in $I_s(\Phi_x)$, occur when $\Phi_x=\pm\Lambda I_c$.

Although the behavior of single weak link SQUID rings (as shorted turns) can be monitored at any nonzero frequency, most studies have been carried out at radio frequency (typically ≈20 MHz) for which a wide range of high-performance electronics is available. We have adopted this frequency range in the work described here. In practice, signal to noise is improved (as in this work) by driving the SQUID ring through the intermediary of a resonant circuit, almost invariably a parallel *LC* (tank) circuit with a high-quality factor (Q). A schematic of the SQUID ring, inductively coupled to an rf tank circuit (with parallel inductance and capacitance L_t and C_t, respectively), is shown in Fig. 1. In the most commonly used experimental scheme the dynamical behavior of the ring is followed in the time domain through the so-called SQUID magnetometer characteristics. In these, the rf voltage ($V_{\rm out}$) developed across the tank circuit is plotted as a function of the rf current ($I_{\rm in}$) used to excite it, where $I_{\rm in}$ is linearly amplitude modulated in time (Fig. 1). This current generates an rf flux (peak amplitude φ) in the tank circuit inductor (coil), a fraction of which ($\mu=M/L_t$ for a coil-ring mutual inductance of M) then couples to the SQUID ring. The supercurrent response in the ring then back-reacts on the tank circuit, and so on. Any addi-

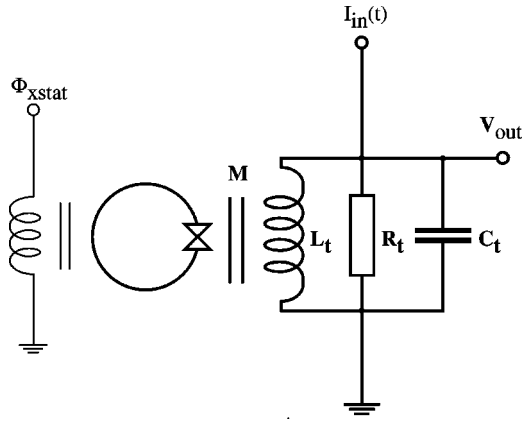

FIG. 1. Schematic of the inductively coupled SQUID ring-tank circuit system.

*Electronic address: t.d.clark@sussex.ac.uk

 ©2001 The American Physical Society

tional static or quasistatic magnetic flux (Φ_{xstat}) that is required is usually supplied via a second coil coupled to the SQUID ring, again as depicted in Fig. 1. For small β values (i.e., from <1 to a few) the V_{out} vs I_{in} dynamics contain as their main element a set of voltage features repeated periodically in I_{in} at intervals $\propto \Phi_o/\Lambda$. The precise form of the SQUID magnetometer characteristics depends both on the type of rf detection employed (e.g., phase sensitive or diode) and the value of Φ_{xstat}.

The nonlinear screening current response can also be made manifest in the frequency domain. This can be accomplished at a fixed level of (peak amplitude) rf flux $\mu\varphi$ at the SQUID ring, without the need for amplitude modulation. For example, in the inductive regime, with β very close to one from below, we have demonstrated that, at sufficiently large values of $\mu\varphi$, fold bifurcations develop in the resonance line shape of a SQUID-ring–tank-circuit system. Indeed, using a bidirectional sweep (up and down in frequency), and at certain values of $\mu\varphi$ and Φ_{xstat}, the system can even display opposed (hammerhead) fold bifurcations in this line shape, one on each side of the resonance [7]. Opposed bifurcations are not only most unusual but, to our knowledge, the possibility of their existence is scarcely mentioned in the literature on nonlinear dynamics [8]. In the case of the inductive SQUID ring, with β very close to one, we have found that these bifurcations are always well separated in frequency. However, in this work we will show that in the weakly hysteretic regime of SQUID behavior ($\beta \approx$ few) this separation can become extremely, perhaps vanishingly, small. Throughout this work we shall term this a pinch resonance.

The one sided (above or below resonance) weak fold bifurcation [9] is taken as the text book example of the onset of nonlinear behavior in a strongly driven oscillator. The development of opposed fold bifurcations (on both sides of the resonance) in any nonlinear system is another matter altogether. As far as we are aware, opposed fold bifurcations had not be seen experimentally prior to our report of hammerhead resonances in the frequency domain of coupled inductive SQUID-ring–tank-circuit systems [7], and only once in the theoretical literature [8]. In itself, we consider that this constitutes a significant contribution to the body of knowledge concerning nonlinear dynamical systems. That the cosine nonlinearity of the SQUID ring can also generate, in part of its parameter space, something as exotic a pinch resonance is simply remarkable, particularly since such resonances appear as solutions to the established equations of motion for the ring-tank system in the weakly hysteretic regime. What this result, and others, point to is that the nonlinear dynamics of SQUID rings coupled to other, linear, circuits is likely to prove very rich indeed [10], more so since the parameter space that has so far been explored is still very limited. As such, these coupled systems are likely to continue to be a focus of attention by the nonlinear community, both in theory and experiment.

With the SQUID ring treated, as in this paper, quasiclassically, there would appear to be many potential applications of its intrinsic nonlinear nature when coupled to external circuits, for example, in logic and memory (single [11] or multilevel [12]), stochastic resonance [13] and in safe communication systems based on chaotic transmission/reception [14]. However, in the last few years there has been a burgeoning interest in exploring the properties of SQUID rings in the quantum regime for use in quantum technologies, particularly for the purposes of quantum computing and quantum encryption [15–18]. This interest has been boosted by recent experimental work on quantum superposition of states in weak link circuits [19–22] and very strongly in the last year by reports in the literature of experimental investigations of superposition states in SQUID rings [23,24]. Quantum technologies will, of necessity, involve time-dependent superpositions for their operation. Where quantum circuits such as SQUID rings are involved, this means the interaction with external electromagnetic (em) fields or oscillator circuit modes. Correspondingly, the effect of applied em fields (classical or quantum) of high enough frequency and amplitude is to generate quantum transition regions where energy is exchanged between the ring energy levels. Given the cosine term in the SQUID ring Hamiltonian [6], these energy exchanges in general involve (nonperurbatively) coherent multiphoton absorption or emission processes [25,26]. These exchange regions extend over very small ranges in the static magnetic flux Φ_{xstat} applied to the ring (typically over $10^{-3}\Phi_o$ to $10^{-4}\Phi_o$), comparable to the width of the anticrossing regions reported in the recent experiments on superposition of states in SQUID rings [23,24]. Such narrow flux widths imply the concomitant existence of extremely strong nonlinearities in the screening supercurrents flowing in the ring. In general these current nonlinearities generate nonlinear dynamical behavior in external (classical) circuits used to probe the superposition state of the ring. As we have emphasized in previous publications [27–29], following these nonlinear dynamics is one way of extracting information concerning the quantum state of a SQUID ring, or any other quantum circuit based on weak link devices. From our perspective, therefore, it is of clear importance to the future development of quantum technologies based on SQUID rings and related devices that these nonlinear dynamics be studied in great detail. Given the results presented in this paper, the nonlinear dynamics of coupled SQUID-ring–probe-circuit systems can display rich and yet unanticipated behavior. With these rings operating in the quantum regime this is even more likely to be the case.

II. EXPERIMENTAL PINCH RESONANCES

Although sometimes unappreciated, probing the nonlinear dynamical behavior of SQUID-ring–tank-circuit systems makes strong demands on the high-frequency electronics used. In order to open up new nonlinear phenomena in these systems we required rf electronics that combined ultra-low-noise performance, large dynamic range, and high slew rate capability. In practice we achieved this by using a liquid-helium cooled (4.2 K), GaAs FET-based, rf amplifier (noise temperature $\lesssim$10 K, gain close to 20 dB) followed by a state of the art, low noise, room-temperature rf receiver. With these electronics we could choose diode or phase sensitive detection of V_{out}. Since phase sensitive detection generally provides better signal to noise, this was always our chosen

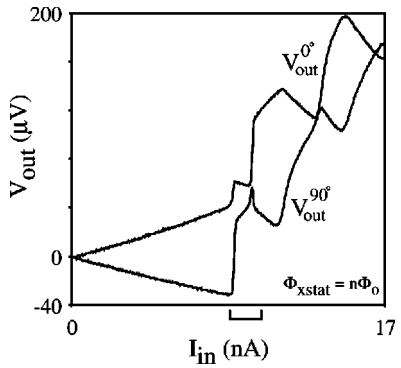

FIG. 2. Experimental equal amplitude (phase sensitive detected and 90° apart in phase) rf SQUID magnetometer characteristics ($V_{\rm out}$ vs $I_{\rm in}$) of a weakly hysteretic ($\beta=2.26$) niobium point contact SQUID ring at a static flux bias of $\Phi_{\rm xstat}=n\Phi_o$. Here, $\Lambda=6\times10^{-10}$ H, $\omega_{\rm in}/2\pi=20.122$ MHz, $L_t=6.3\times10^{-8}$ H, $Q=1058$, $K^2=4\times10^{-3}$ and $T=4.2$ K.

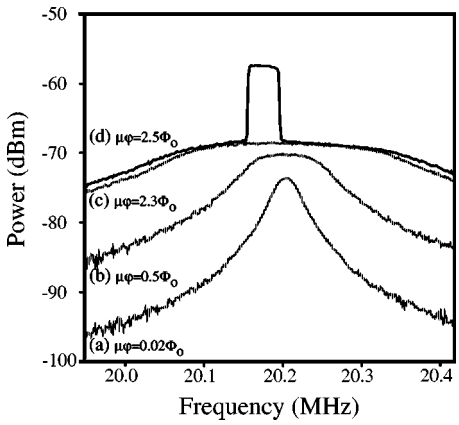

FIG. 3. (a) to (d) $T=4.2$ K, $\Phi_{\rm stat}=(n+1/2)\Phi_o$ plots of the unidirectional frequency sweeps (from low to high) for the weakly hysteretic ($\beta=2.26$) ring–tank-circuit system of Fig. 2 for different peak rf flux amplitudes at the SQUID ring (i.e., $\mu\varphi=0.02\Phi_o$, $0.5\Phi_o$, $2.3\Phi_o$, and $2.5\Phi_o$) showing the punch through at higher amplitude (e.g., $\mu\varphi\gtrsim2\Phi_o$).

mode of operation for acquiring SQUID magnetometer characteristics.

In the work reported in this paper the SQUID rings used were of the Zimmerman two hole type [30]. These were fabricated in niobium with a niobium weak link of the point contact kind. This weak link was formed by mechanical adjustment between a point and a post screw, the latter having a plane machined end face that had been preoxidized prior to its insertion in the SQUID block. The weak link was made *in situ* at 4.2 K via a room temperature adjustment mechanism. As we have shown in previous publications [7], the control we can exert using this mechanism is very good, sufficient in fact to make reproducible point contact SQUID rings with any desired β value from inductive [7] to highly hysteretic [12].

In Fig. 2 we show what we term the equal amplitude magnetometer characteristics for a weakly hysteretic (β close to 2) niobium point contact SQUID ring coupled to an rf tank circuit. In these characteristics, taken at 4.2 K with a static bias flux of $n\Phi_o$, the frequency of the drive current was set to the coupled SQUID-block–tank-circuit resonant frequency before a weak link contact was made (i.e., $\omega_{\rm in}/2\pi$) and the voltage components ($V_{\rm out}^{0^\circ}$ and $V_{\rm out}^{90^\circ}$) were maintained exactly 90° out of phase. However, their relative phases with respect to $I_{\rm in}$ were rotated electronically until the average slopes of the two characteristics are essentially equal. This approach was adopted for convenience—it presented the periodic features in $I_{\rm in}$ of the orthogonal phase components of $V_{\rm out}$ at essentially the same amplitude. Here, the (measured) ring inductance $\Lambda=6\times10^{-10}$ H, the measured ring-tank circuit coupling coefficient $K^2(=M^2/\Lambda L_t)=0.004$, $L_t=6.3\times10^{-8}$ H, $Q=1058$, and the drive (excitation) frequency for $I_{\rm in}$, $\omega_{\rm in}/2\pi=20.122$ MHz. It is apparent from Fig. 2 that even in this weakly hysteretic regime the observed SQUID magnetometer characteristics are highly nonlinear and contain a wealth of detail.

Some of the time domain information of Fig. 2 can be recast in a quite dramatic form in the frequency domain. To extract this experimentally requires the use of a high-performance spectrum analyzer with a tracking generator output [7]. This output provides a voltage signal of constant peak-to-peak amplitude over the frequency range of interest. Feeding this through a series high impedance generates an rf current in the tank circuit which, in turn, creates an rf flux (peak amplitude $\mu\varphi$) at the SQUID ring. As with our previous work on SQUID-ring–tank-circuit dynamics in the inductive regime [5,7], the details of this behavior depend crucially on the value of the static bias flux $\Phi_{\rm xstat}$.

In Fig. 3 we show four frequency responses for unidirectional sweeps, from low to high frequency, for the SQUID-ring–tank-circuit system of Fig. 2 (at $T=4.2$ K). The data were taken at rf flux amplitudes $\mu\varphi$ ranging from $0.02\Phi_o$, to $2.5\Phi_o$, with $\Phi_{\rm xstat}=(n+1/2)\Phi_o$. These frequency responses were recorded using a high-performance, but conventional, commercial spectrum analyzer (a Rohde and Schwarz FSAS system) that could only scan in this unidirectional manner. What is clear from Fig. 3 is that as $\mu\varphi$ becomes a significant fraction of a flux quantum the line shape of the frequency response curves changes dramatically. In particular, for $\mu\varphi\gtrsim2\Phi_o$ there is a punch through effect that leads to the creation of fold-bifurcation cuts. If we refer back to Fig. 2, this value of peak rf flux $\mu\varphi$ equates to a drive current corresponding to the feature shown bracketed in Fig. 2, but for the case of static bias flux $\Phi_{\rm xstat}=(n+1/2)\Phi_o$. The significance of this was revealed when bidirectional frequency sweeps (from low to high and then high to low) were taken using a spectrum analyzer of our own design. This spectrum analyzer is shown in block form in Fig. 4. As an illustration of its utility, we show in Fig. 5 the result of this bidirectional sweep for the curve (d) of Fig. 3 ($\mu\varphi=2.5\Phi_o$), again at $\Phi_{\rm xstat}=(n+1/2)\Phi_o$. As can be seen in Fig. 5, there are four fold-bifurcation cuts, one each at the lowest and highest frequency excursions in the response, and two inner cuts, one on the sweep up and the other on the sweep down. Within the experimental resolution, as reflected in the data points, these inner cuts appear to overlay exactly. To our knowledge, this has not been observed before. For

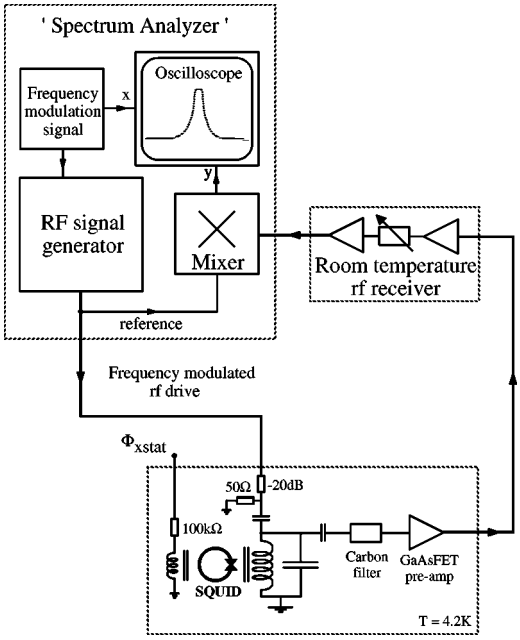

FIG. 4. Block diagram of the spectrum analyzer used to record the bidirectional frequency response curves of Fig. 5.

this bidirectional response it seems reasonable to adopt the description pinch resonance.

The frequency response curve of Fig. 5 and those plotted in Fig. 3 as a function of coupled rf amplitude, are perfectly typical of the low β value ($\approx$few) hysteretic SQUID-ring–tank-circuit systems that we have studied. To aid in interpretation we have provided in Fig. 6 a schematic of three different bidirectional frequency response curves: (a) where the inner pair of opposed fold-bifurcation cuts are well separated in frequency, (b) where these cuts superimpose in frequency (i.e., in our terminology, a pinch resonance), and (c) where the fold bifurcations have moved beyond one another. It seems clear that the data of Fig. 5 correspond to the bidirectional response of Fig. 6(b) since this response can obviously be differentiated from those of Figs. 6(a) and 6(c). It is interesting to note that the existence of any one of the bidirectional response curves shown schematically in Fig. 6 could not be revealed using standard commercial spectrum analyzers since these always sweep the frequency unidirectionally, i.e., from low to high. For completeness, we show in Fig. 7 the bidirectional frequency responses (with both up and down sweeps) for the ring-tank circuit system of Fig. 3(d) and 5 ($T=4.2$ K, $\mu\varphi=2.5\Phi_o$) at the static bias flux values

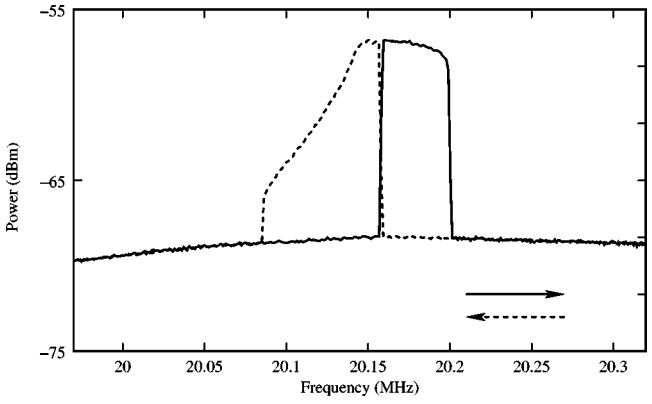

FIG. 5. Expanded, bidirectional, frequency sweeps (low to high and then high to low) for the response (d) in the data of Fig. 3, again with $\mu\varphi=2.5\Phi_o$ and $T=4.2$ K. This value of peak $\mu\varphi$ equates to a drive current, at static bias flux $\Phi_{xstat}=(n+1/2)\Phi_o$, corresponding to the feature shown bracketed in Fig. 2.

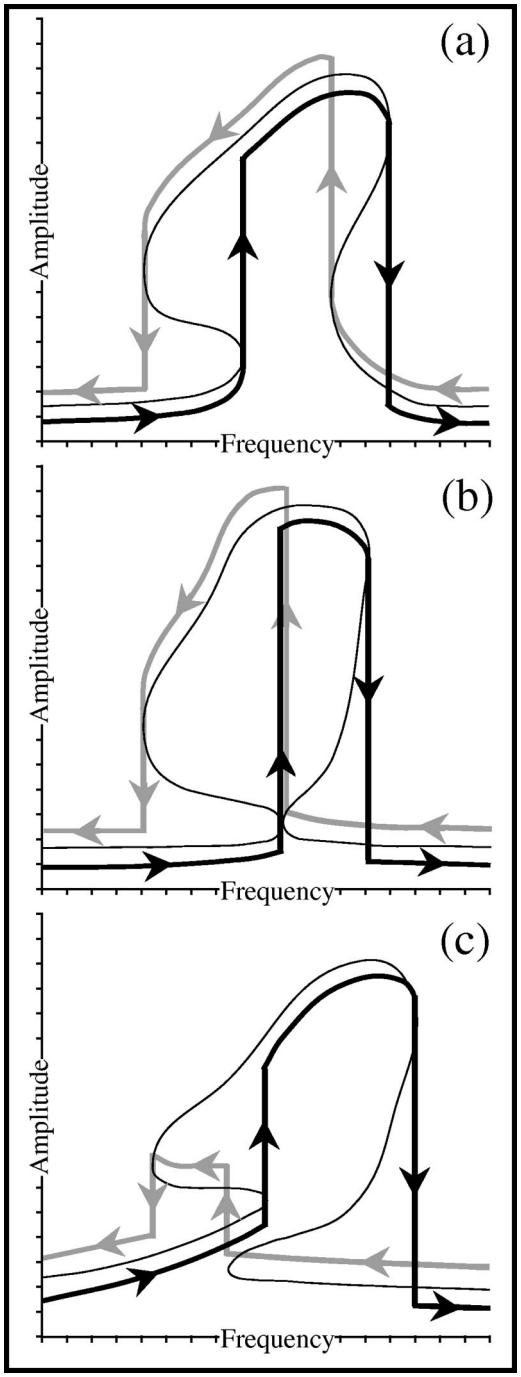

FIG. 6. A schematic of three different bidirectional frequency response curves: (a) where the inner pair of opposed fold-bifurcation cuts are well separated in frequency, (b) where these cuts superimpose in frequency (a pinch resonance), and (c) where the fold bifurcations have moved beyond one another.

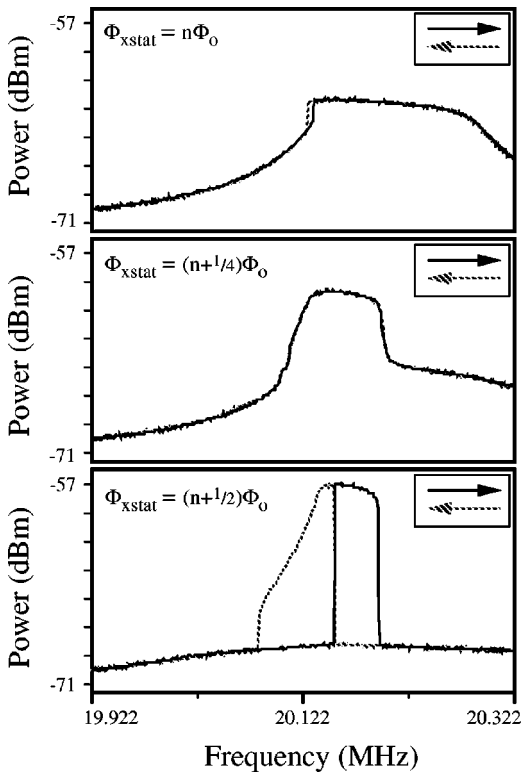

FIG. 7. Experimental bidirectional frequency response curves for the SQUID-ring–tank-circuit system of Fig. 3(d) and 5 ($T=4.2$ K, $\mu\varphi=2.5\Phi_o$) at three values of static bias flux at the ring $\Phi_{xstat}=n\Phi_o$, $(n+1/4)\Phi_o$, and $(n+1/2)\Phi_o$.

$\Phi_{xstat}=n\Phi_o$, $(n+1/4)\Phi_o$, and $(n+1/2)\Phi_o$. As is apparent, the pinch resonance can only be seen in one of these responses, i.e., at $\Phi_{xstat}=(n+1/2)\Phi_o$.

III. THEORETICAL MODEL

A. RSJ+C description

In the standard dynamical description of a SQUID ring it is customary to invoke the well-known (quasiclassical) resistively shunted junction plus capacitance (RSJ+C) model [4] of the weak link in the ring. Here, a pair (Josephson) current channel is in parallel with an effective weak link capacitance C and a normal current channel of resistance R. For an applied current $I>I_c$, the normal channel opens up with a value of R that is characteristic of the particular weak link in the ring. In this (and other) models the SQUID ring moves in the space of total included magnetic flux $\Phi=\Phi_x+\Lambda I_s$ with an effective mass given by the weak link capacitance (C). Within the RSJ+C model it is always assumed that the SQUID ring can be treated as a quasiclassical object, such that C is relatively large, typically $\approx 10^{-13}$ to 10^{-14} F.

In the RSJ+C description the SQUID ring and tank circuit constitute a system of coupled oscillators with equations of motion that can be written in the form

$$\text{tank circuit:}\quad C_t\ddot{\varphi}+\frac{\dot{\varphi}}{R_t}+\frac{\varphi}{L_t}=I_{\text{in}}+\frac{K^2\Phi}{M(1-K^2)}, \tag{1}$$

where R_t is the tank circuit resistance on parallel resonance of the coupled system and I_{in} is the drive current (Fig. 1), which may contain both coherent and noise contributions.

$$\text{SQUID ring:}\quad C\ddot{\Phi}+\frac{\dot{\Phi}}{R}+\frac{\Phi}{\Lambda(1-K^2)}+I_c\sin\left(\frac{2\pi\Phi}{\Phi_0}\right)=\frac{K^2\varphi}{M(1-K^2)}, \tag{2}$$

where $I=I_c\sin(2\pi\Phi/\Phi_0)$ is the phase-dependent Josephson current for the weak link in the ring.

Until recently little effort appears to have been directed to solving the coupled equations in their full nonlinear form, understandably given the level of computational power required to deal with them. Instead it has often been assumed that it is sufficiently accurate to linearize the SQUID ring equation of motion. This is equivalent to invoking the adiabatic condition that the ring stays at, or very close to, the minimum in its potential

$$U(\Phi,\Phi_x)=\frac{(\Phi-\Phi_x)^2}{2\Lambda}-\frac{I_c\Phi_o}{2\pi}\cos\left(\frac{2\pi\Phi}{\Phi_o}\right) \tag{3}$$

as this varies with time. The SQUID equation (2) then reduces to

$$I_c\sin\left(\frac{2\pi\Phi}{\Phi_o}\right)+\frac{\Phi}{\Lambda(1-K^2)}=\frac{K^2\varphi}{M(1-K^2)}. \tag{4}$$

However, as we have shown in a recent work [12], this approximation should be treated with great care, particularly in the hysteretic regime of behavior. In order to avoid this problem we have chosen to solve the full coupled equations of motion [(1) and (2)] for the system using values of C and R considered typical of a weakly hysteretic SQUID ring. We shall demonstrate that pinch resonances, such as those we have presented in Fig. 5, and which match with the experimentally determined circuit parameters, show up as solutions of these equations.

B. Pinch resonances

With a knowledge of the system parameters, and an estimate of I_c, we can solve the coupled equations of motion (1) and (2) numerically to find the value, at a given Φ_{xstat}, of the rf tank circuit voltage $\dot{\varphi}$ as a function of the frequency of the fixed amplitude sinusoidal drive current I_{in}. This voltage response can then be used to compute the bidirectional frequency responses of the ring–tank-circuit system. To do this we considered an interval $[\omega_{\min}/2\pi$ to $\omega_{\max}/2\pi]$ in the drive frequency that contained the (peak amplitude) resonant frequency of the system. This interval was divided into N bins that gave us a resolution of $\delta\omega=(\omega_{\max}-\omega_{\min})/N$ in the frequency domain. We then drove the tank circuit at ω_{in} (for $I_{\text{in}})=\omega_{\min}+n\delta\omega$ for $n=0,1,\ldots,N$ increments in frequency (this being done without changing the initial conditions of

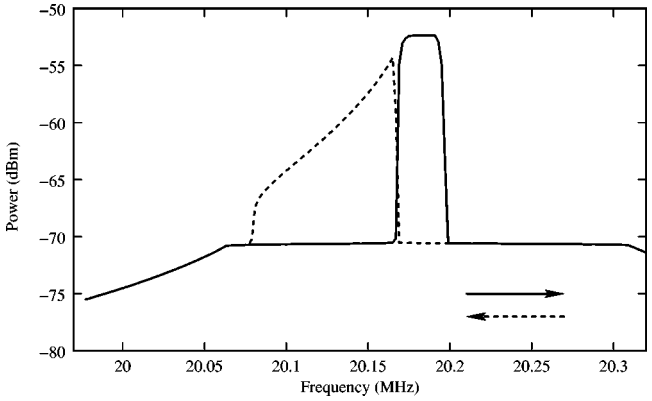

FIG. 8. Computed (RSJ+C model) bidirectional, frequency response curves (low to high and then high to low) using the ring and tank circuit parameters of Figs. 2 and 5 with $I_c = 1.23\ \mu$A, $C = 10^{-14}$ F and $R = 100\ \Omega$ ($CR = 10^{-12}$ sec).

the system), thus obtaining the power in the tank circuit at each of these frequencies via [5,7]

$$P(\omega_{\rm in}) = \frac{2}{(2\pi m/\omega_{\rm in})} \left| \int_o^{2\pi m/\omega_{\rm in}} \dot{\varphi} \exp(i\omega_{\rm in} t)\, dt \right|^2 \qquad (5)$$

for a given integer m. We note that m is taken so that the power is integrated over a few Q cycles of the tank circuit oscillation to reduce the effects of transients. In the situation where the nonlinearities in the coupled ring–tank-circuit system are strong, and where, typically, the rf drive amplitudes are large, we have already shown [5,7] that fold-bifurcation regions (i.e., regions where more than one stable solution exists) can develop in the resonance curves of the system.

To make a comparison with the experimental data of Fig. 5 we estimated the value of the β parameter from the 0° SQUID magnetometer characteristic of Fig. 2 using the ratio (on the current axis $I_{\rm in}$) of the initial riser to the interval between the periodic features in this characteristic. This yielded a β value of 2.26, which, for a ring inductance of 6×10^{-10} H, set $I_c = 1.23\,\mu$A. In a recent publication we described a quantum electrodynamic model [31] of a SQUID ring that has allowed us to derive an expression for the effective ring capacitance (C), knowing the superconducting material from which it is constructed and the value of the weak link critical current. With niobium as the material, and $I_c \cong 1$ to a few μA, this yields $C \lesssim 10^{-14}$ F. An alternative model [32], using a different approach, gives rise to similar size capacitances. From the literature [32,33], a corresponding effective dissipative resistance in the ring $\approx 100\ \Omega$ appears perfectly reasonable, setting a ring CR time constant of 10^{-12} sec.

The theoretical bidirectional frequency response curves corresponding to the experimental data (and circuit parameters) of Fig. 5 are shown in Fig. 8, with I_c and CR taken to be 1.23 μA and 10^{-12} sec, respectively. These were computed, sweeping forwards and backwards across the defined frequency window, using a 4th order Runge-Kutta-Merson routine with adaptive step size error control. The SQUID-ring–tank-circuit coupling (K^2) and Q parameters were set as for Figs. 3(d) and 5 together with $\mu\varphi = 2.5\Phi_o$ and $\Phi_{\rm xstat} = (n + 1/2)\Phi_o$. From numerous computations we have found that the shape of the bidirectional response in this RSJ+C approach is determined principally by the CR product and is only weakly dependent on the particular values of C and R chosen, at least in the ranges 10^{-12} to 10^{-14} F and 1 to 100 Ω. With the circuit parameters detailed above, we found that the best fit to Fig. 5 (the pinchoff resonance) is made with $CR = 10^{-12}$ sec. As for the experimental data displayed in Fig. 5, the theoretical inner fold-bifurcation cuts superimpose very well, at least to the limits of our computational accuracy. This is reflected in the computed data points in the region of these inner cuts.

Clearly, the correspondence between the theoretically calculated response curves of Fig. 8 and the experimental bidirectional responses of Fig. 5 is good, both in frequency range and line shape. For example, at $\Phi_{\rm xstat} = (n + 1/2)\Phi_o$ the experimental and theoretical responses appear to meet exactly at one point in the frequency domain. However, we must caution that due to the numerical nature of the calculation it is not possible theoretically to prove that this single frequency meeting point is exact. Nevertheless, by trying different amplitudes for $I_{\rm in}$ we have found that we can narrow the separation between the solutions down to an arbitrarily small level. This reflects the situation found experimentally. We note that we have been unable to generate this theoretical fit to our experimental bidirectional response curves using the linearized SQUID equation (4).

With regard to the alternative frequency response curves of Fig. 6, and the experimental data of Figs. 5 and 7, we note that it may be appropriate to treat this weakly hysteretic SQUID-ring–tank-circuit system as an extremely sensitive finite state machine [34]. If so, we may be able to compare the transition state diagram for the different cycles shown in Figs. 6(a), 6(b), and 6(c). As an example, we may ask whether it is possible in the pinch resonance (b) to go between the lower left and lower right branches without jumping up to the loop. This could happen occasionally but still be beyond the sensitivity limits of our present experimental apparatus. If it does occur there will be a sharp transition between the full pinch loop resonance [fine black line in Fig. 6(b)] and the resonance displaying sets of bifurcation cuts, i.e., in the one case the resonance loop is not accessed, in the other (the latter) it is. In principle, the two processes could be distinguished since the pathways around the loop involve very much larger voltages than the crossing between the lower branches of the resonance. Such contrasting processes would, of course, be of scientific interest but could also have potential in device applications.

IV. CONCLUSIONS

In this paper we have shown that a single weak link SQUID ring, weakly hysteretic and coupled to a simple parallel resonance tank circuit, can display quite remarkable, and previously unexpected, nonlinear behavior in the frequency domain. Thus, we have demonstrated that this system exhibits opposed fold-bifurcation cuts in its bidirectional fre-

quency response curves which, at specific values of rf and static bias flux, and within our experimental resolution, superimpose exactly. Since single fold bifurcations in the upper or lower branches of a strongly driven resonant system are usually taken as one of the standard examples of the onset of nonlinear dynamics [9], the onset of opposed fold bifurcations is of special note. That this can result, as a limiting case, in the creation of a pinch resonance would appear to be exceptional and, in our opininion, of very considerable interest to the nonlinear community. Nevertheless, as we have also shown, such pinchoff resonances can be modeled well within the full, nonlinear RSJ+C description of the ring–tank-circuit system. Together with other recently published work [12], these results would appear to suggest that there is still a great deal to be explored in the nonlinear dynamics of SQUID-ring–resonator systems in the quasiclassical regime. It is also apparent that the new nonlinear dynamical results obtained in this regime point to future research needed to implement quantum technologies based on SQUID rings (and related weak link devices) interacting with classical probe circuits [5,7,30]. From both perspectives it is clear that the SQUID ring which, through the cosine term in its Hamiltonian, is nonlinear to all orders, is set to continue to reveal new and interesting nonlinear phenomena of importance in the field of nonlinear dynamics and in the general area of the quantum-classical interface as related to the measurement problem in quantum mechanics. It is also apparent that in both the classical and quantum regimes the nonlinear dynamics generated in coupled circuit systems involving SQUID rings could form the basis for new electronic technologies.

ACKNOWLEDGMENT

We would like to thank the Engineering and Physical Sciences Research Council for its generous funding of this research.

[1] W. C. Schieve, A. R. Bulsara, and E. W. Jacobs, Phys. Rev. A **37**, 3541 (1988).
[2] A. R. Bulsara, J. Appl. Phys. **60**, 2462 (1986).
[3] M. P. Soerensen, M. Barchelli, P. L. Christiansen, and A. R. Bishop, Phys. Lett. **109A**, 347 (1985).
[4] K. K. Likharev, *Dynamics of Josephson Junctions and Circuits* (Gordon and Breach, Sidney, 1986).
[5] T. D. Clark, J. F. Ralph, R. J. Prance, H. Prance, J. Diggins, and R. Whiteman, Phys. Rev. E **57**, 4035 (1998).
[6] T. P. Spiller, T. D. Clark, R. J. Prance, and A. Widom, Prog. Low Temp. Phys. **13**, 219 (1992).
[7] R. Whiteman, J. Diggins, V. Schöllmann, T. D. Clark, R. J. Prance, H. Prance, and J. F. Ralph, Phys. Lett. A **234**, 205 (1997).
[8] A. H. Nayfeh, S. A. Nayfeh, and M. Pakdemirli, in *Non-Linear Dynamics and Stochastic Mechanics*, edited by W. Kleinmann and N. Sri Namachchivaya (CRC, Boca Raton, FL, 1995), p. 190.
[9] L. D. Landau and E. M. Lifshitz, *Mechanics—Course in Theoretical Physics* (Pergamon, Oxford, 1987), Vol. 1, p. 89.
[10] See, for discussions of bifurcations, etc., in nonlinear systems, D. Zwillinger, *Handbook of Differential Equations* (Academic, Boston, 1992), p. 16; S. H. Strogatz, *Non-Linear Dynamics and Chaos* (Perseus Books, Reading, MA, 1994), p. 44.
[11] See V. P. Koshelets, K. K. Likharev, and V. V. Migulin, IEEE Trans. Magn. **23**, 755 (1987); H. Miyake, N. Fukaya, and Y. Okabe, *ibid.* **21**, 578 (1985).
[12] R. J. Prance, R. Whiteman, T. D. Clark, H. Prance, V. Schöllmann, J. F. Ralph, S. Al-Khawaja, and M. Everitt, Phys. Rev. Lett. **82**, 5401 (1999).
[13] See, for example A. R. Bulsara, and L. Gammaitoni, Phys. Today **49** (3), 39 (1996); L. Gammaitoni, P. Hänggi, P. Jung, and F. Marchesoni, Rev. Mod. Phys. **70**, 1 (1998).
[14] See, for example, M. Hasler, Int. J. Bifurcation Chaos Appl. Sci. Eng. **8**, 647 (1998).
[15] See, for example, *Introduction to Quantum Computation and Information*, edited by H. K. Lo, S. Popescu, and T. P. Spiller (World Scientific, Teaneck, NJ, 1998).
[16] T. P. Orlando, J. E. Mooij, L. Tian, C. H. van der Wal, L. S. Levitov, S. Lloyd, and J. J. Mazo, Phys. Rev. B **60**, 15 398 (1999).
[17] Y. Makhlin, G. Schön, and A. Shnirman, Nature (London) **398**, 305 (1999).
[18] D. Averin, Nature (London) **398**, 748 (1999).
[19] R. Rouse, S. Han, and J. E. Lukens, Phys. Rev. Lett. **75**, 1614 (1995).
[20] P. Silvestrini, B. B. Ruggiero, C. Granata, and E. Esposito, Phys. Lett. A **267**, 45 (2000).
[21] Y. Nakamura, C. D. Chen, and J. S. Tsai, Phys. Rev. Lett. **79**, 2328 (1997).
[22] Y. Nakamura, Y. A. Pashkin, and J. S. Tsai, Nature (London) **398**, 786 (1999).
[23] J. R. Friedman, V. Patel, W. Chen, S. K. Tolpygo, and J. E. Lukens, Nature (London) **406**, 43 (2000).
[24] C. H. van der Wal, A. C. J. ter Haar, F. K. Wilhem, R. N. Schouten, C. J. P. M. Harmans, T. P. Orlando, S. Lloyd, and J. E. Mooij, Science **290**, 773 (2000).
[25] T. D. Clark, J. Diggins, J. F. Ralph, M. J. Everitt, R. J. Prance, H. Prance, R. Whiteman, A. Widom, and Y. N. Srivastava, Ann. Phys. **268**, 1 (1998).
[26] M. J. Everitt, P. Stiffell, T. D. Clark, A. Vourdas, J. F. Ralph, H. Prance and R. J. Prance, Phys. Rev. B (to be published 2001).
[27] R. Whiteman, V. Schöllmann, M. Everitt, T. D. Clark, R. J. Prance, H. Prance, J. Diggins, G. Buckling, and J. F. Ralph, J. Phys.: Condens. Matter **10**, 9951 (1998).
[28] T. D. Clark, J. F. Ralph, R. J. Prance, H. Prance, J. Diggins, and R. Whiteman, Phys. Rev. E **57**, 4035 (1998).
[29] R. Whiteman, T. D. Clark, R. J. Prance, H. Prance, V. Schöllmann, J. F. Ralph, M. Everitt, and J. Diggins, J. Mod. Opt. **45**, 1175 (1998).
[30] J. E. Zimmerman, P. Thiene, and J. T. Harding, J. Appl. Phys. **41**, 1572 (1970).
[31] J. F. Ralph, T. D. Clark, J. Diggins, R. J. Prance, H. Prance,

and A. Widom, J. Phys.: Condens. Matter **9**, 8275 (1997).
[32] K. Gloss and F. Anders, J. Low Temp. Phys. **116**, 21 (1999).
[33] J. E. Zimmerman, *Proceedings of 1972 Applied Superconductivity Conference, Annapolis* (IEEE Publications, New York, 1972), pp. 544–561.
[34] R. P. Feynman, *Feynman Lectures on Computation*, edited by A. J. G. Hey and R. W. Allen (Penguin, London, 1999), p. 55.